

Tunable optical buffer through an analogue to Electro-magnetically Induced Transparency in coupled Photonic Crystal cavities

Changyu Hu,^{*,†} Sebastian A. Schulz,^{‡,‡,¶} Alexandros A. Liles,[†] and Liam O'Faolain^{†,‡,¶}

[†]*School of Physics and Astronomy, SUPA, University of St Andrews, St Andrews, UK*

[‡]*Centre for Advanced Photonics and Process Analysis, Cork Institute of Technology, Cork, Ireland*

[¶]*Tyndall, National Institute, Cork, Ireland*

E-mail: ch236@st-andrews.ac.uk

Abstract

Tunable on-chip optical delay has long been a key target for the research community, as it is the enabling technology behind delay lines, signal re-timing and other applications vital to optical signal processing. To date the field has been limited by high optical losses associated with slow light or delay structures. Here, we present a novel tunable delay line, based on a coupled cavity system exhibiting an Electro-magnetically Induced Transparency-like transmission spectrum, with record low loss, around 15dB/ns. By tuning a single cavity the delay of the complete structure can be tuned over 120ps, with the maximum delay approaching 300ps.

Keywords

Slow light, Photonic Crystal, Optical delay lines, nanophotonics, optical cavities, electromagnetically induced transparency

Slow light structures have potential for applications such as optical buffers and delay lines.^{1,2} Integrated optical delay lines are an important component of optical signal processing systems and are required for a range of functionalities, e.g. bit swapping or signal re-timing. Despite significant early progress on integrated delay lines based on photonic crystal waveguides and coupled cavity structures³⁻⁶ significant challenges remain. It is now widely accepted that current delay lines are generally limited by the propagation loss in the structure, rather than by group velocity dispersion.⁷⁻⁹ Significant work has gone into optimising both silicon based coupled oscillator waveguides and slow light photonic crystals, e.g. by Minkov and Savona,¹⁰ with problems relating to backscattering understood and minimised. Nonetheless, the high refractive index contrast of the latter (i.e. Photonic Crystals), which enables a small footprint, amplifies the effects of roughness placing a limit on the minimum propagation loss that can be achieved - with 35dB/ns being the current record.⁶ Spiral waveguides can achieve large delays with a small footprint, but such structures lack dynamic control of the delay. After a spiral is fabricated the delay is fixed, ruling it out for applications such as signal re-timing or on-demand release of signals. Low loss tunable delays have been demonstrated using silicon, rib waveguide based Bragg gratings,¹¹ achieving a loss per delay of approximately 20dB/ns. This work showed very good propagation losses but a relatively large footprint and therefore large power consumption during active tuning.

It is crucial that delay lines are realised that are compact, low loss and tunable. Here, we present a novel approach to optical buffers, that combines low loss polymer waveguides with photonic crystal cavities. As we will describe in the Theory section, the cavities show behaviour analogous to electromagnetically induced transparency (EIT), resulting in large, and dynamically controllable optical delay, similar to Xu et al.¹² Our system has the important difference in that the light spends a significant percentage of the time traveling in

the polymer waveguides, which has lower propagation loss relative to silicon nanowires, resulting in reduced total loss compared to other on-chip optical delay lines. Specifically, we demonstrate delays as large as 300ps, delay tuning exceeding 120ps and record low optical losses of approximately 15dB/ns. The use of polymer waveguides also increases the coupling efficiency to optical fibres and the fibre to fibre loss of our system can be less than 3 dB.

Theory

Optical resonators are constrained by the delay-bandwidth limit, i.e. the group delay in a resonant system is inversely proportional to the bandwidth. The bandwidth of the resonant system is given by the quality (Q)-factor and is dependent on both the coupling Q-factor and the intrinsic Q-factor, both of which are typically fixed at the design and fabrication stages and are very difficult to tune dynamically. Therefore, a resonant delay system provides a binary delay tuning only - either a signal is on-resonance and experiences the full delay of the system, or it is off-resonance and experiences no delay. We overcome this limitation by designing a coupled resonator system that displays an analogous effect to electromagnetically induced transparency (EIT) and allows for continuous delay tuning. In quantum mechanics, the atom transition in the three energy levels system can be $|1\rangle - |3\rangle$ or $|1\rangle - |3\rangle - |2\rangle - |3\rangle$, which is illustrated in Fig.1. When the associated wavefunctions interfere, the EIT state window appears between $|2\rangle$ and $|3\rangle$. Two resonators with ω_a and ω_b can be represented as the two energy states in atomic transition and an optical analog EIT-like effect can occur, as first proposed by D. D. Smith et al.,¹³ see Fig.1. This EIT-like effect can be obtained through the coherent interference between two resonators connected by an optical path.

Here, we consider a waveguide that is indirectly (vertically or side) coupled to two resonators as in Fig.2. The resonators have resonance frequency ω_a and ω_b , respectively.

Using a transfer matrix method, the transmission spectra of the system can be calculated,

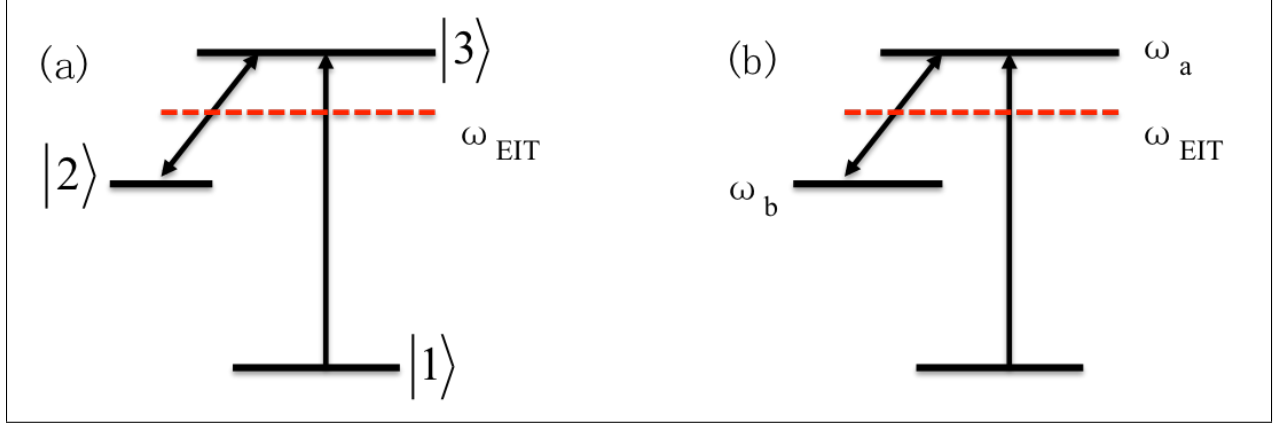


Figure 1: a) EIT in an atomic three-level system. The EIT effect appears between states $|2\rangle$ and $|3\rangle$, when the different excitation pathways interfere destructively. b) Three-level representation of an optical analogue in a system consisting of two coupled resonators.

to quantify the EIT-like properties:

$$|T(\omega)|^2 = \left(\frac{|t_a t_b|}{1 - |r_a r_b|}\right)^2 (1 + 4\left(\frac{\sqrt{|t_a t_b|}}{1 - |r_a r_b|}\right)^2 \sin^2(\theta))^{-1}, \quad (1)$$

where $t_{a,b}$ and $r_{a,b}$ are transmission and reflection matrix coefficients for the two resonators, respectively, given by

$$t_{a,b} = \frac{j(\omega - \omega_{a,b}) + \gamma}{j(\omega - \omega_{a,b}) + \gamma_c + \gamma}, \quad r_{a,b} = \frac{\gamma_c}{j(\omega - \omega_{a,b}) + \gamma_c + \gamma}. \quad (2)$$

Here γ is the amplitude radiative-loss rate, related to the radiative quality factor by $\gamma = \frac{\pi c}{Q_{\text{rad}} \lambda_0}$, $\omega_{a,b}$ is the resonance frequency and γ_c is the total waveguide-resonator coupling rate due to coupling into both cavities. θ is the round-trip phase accumulated and is give by:

$$\theta = \frac{1}{2} \arg[r_a r_b \exp(-2j\beta(\omega)L)], \quad (3)$$

where $\beta(\omega)$ is the waveguide dispersion relation. From eqn.1, the system's group delay is given by:

$$\tau_g(\omega) = \frac{d\text{Arg}[T(\omega)]}{d\omega} = \tau_{g+}(\omega) + \tau_{g,wg}(\omega), \quad (4)$$

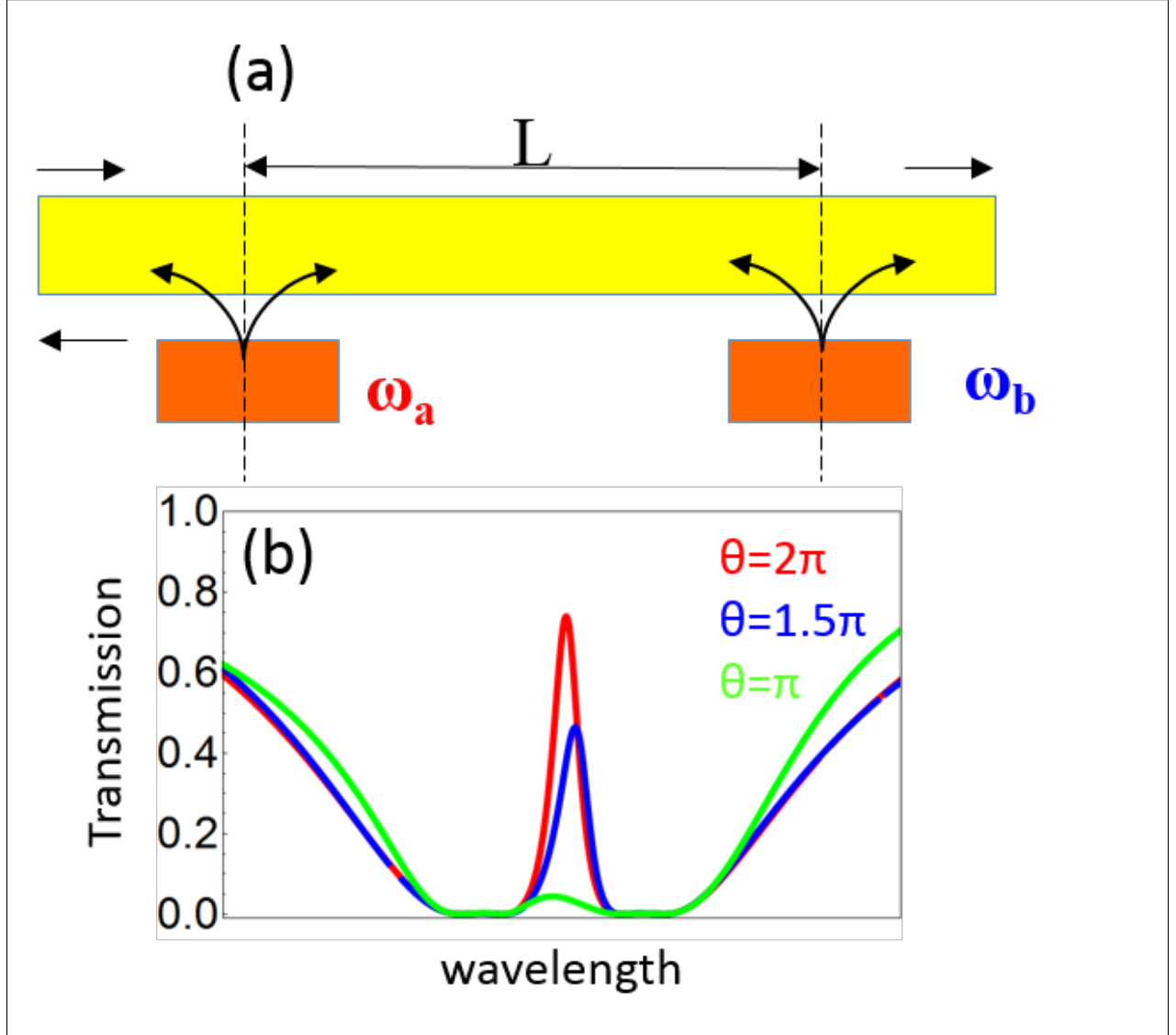


Figure 2: a) Schematic of a coupled cavity system that can slow down light. The smaller rectangles represent the cavities, with resonance frequencies ω_a and ω_b , the large one the waveguide. The cavities are separated by a distance L and couple to each other through the waveguide. b) Response of the system, as computed using coupled mode theory. Three different relative phases are shown. An EIT-like transmission spectrum is observed when $\theta=2\pi$. An intermediate EIT peak, with reduced transmission is observed when $\theta = 1.5\pi$, while the EIT peak is at it minimum when $\theta = \pi$, resulting in an approximately flat-bottomed response.

where $\tau_{g,wg}(\omega)$ is the waveguide group delay, i.e. the delay corresponding to a single, direct pass through the waveguide only and τ_{g+} is the additional delay incurred due to the coupled cavity system. Thus, the system's additional group delay τ_{g+} is obtained from $\tau_{g+}(\omega) = \tau_g(\omega) - \tau_{g,wg}(\omega)$. This delay can significantly exceed the combined delay of the individual elements (i.e. the combined single pass delay of the waveguide and the two cavities) and is dominated by the nature of the interference between the two cavities (acting analogous to the atomic states in EIT).

If we consider a loss-less waveguide, when the θ is $2n\pi$, the coherent interference between the two cavities leads the system represented as an EIT analog spectrum, as shown in Fig.2. b. When the θ is $(2n + 1)\pi$, the EIT analog condition is no longer satisfied in Fig.2.b. The structure instead behaves as a flat-top reflection filter. The properties of the EIT-peak can be controlled through γ_c and γ_{rad} . For a given γ_{rad} and frequency detuning $\delta\omega = \omega_a - \omega_b$, a high γ_c causes a narrow peak with a large delay, but also decreases the transmission of the EIT peak. Conversely, a low γ_{rad} gives a high transmission, but with small delay. For a given γ_c and $\delta\omega$, a low γ_{rad} on the other hand increases both the transmission of the EIT peak and the achievable delay. For very large values of γ_{rad} the EIT peak can disappear completely as insufficient light circulates to fulfill the interference conditions. It is thus advantageous to use cavities with a high intrinsic Q-factor, i.e. a low γ_{rad} . Similarly, a small $\delta\omega$ gives a narrow EIT-like peak with decreased transmission. However, no EIT-like effect is produced when $\delta\omega$ is too large, because excessive $\delta\omega$ causes negligible interference between the two cavity modes.

Fabrication

In this work, we implement the system by coupling two PhC cavities via a polymer (SU8) bus waveguide. The PhC cavities are fabricated in a silicon-on-insulator platform, consisting of a 220nm silicon slab on a $2\mu m$ buried oxide layer. The cavities follow the dispersion adapted

design of reference¹⁴ and are well suited for vertical coupling to polymer waveguides.¹⁵ The PhC cavities have a lattice constant of $a = 390nm$ and a hole radius, $r = 100nm$. The pattern was defined through electron beam lithography and transferred into silicon through reactive ion etching, before being covered in flowable oxide. The oxide backfills the holes and creates a $100nm(\pm 10nm)$ spacer layer between the PhC cavities and the polymer waveguide. This thickness is chosen as it provides efficient coupling between the waveguide and the cavity, while keeping the overall Q-factor, Q_{tot} , high. The polymer waveguides are created through electron beam lithography of SU8, giving a $3\mu m \times 2\mu m$ cross-section. A cleaved side-view scanning electron microscope (SEM) image of the polymer waveguide above a PhC cavity is shown in Fig.3a). A top-view of the dispersion adapted PhC cavity is presented in Fig.3b). Fig.3c shows three coupled cavity systems, with varying cavity separation. For dynamic control of the EIT-like peak, and hence the group index, Ohmic heaters (200nm Ni on 20nm Cr), shown in Fig.3d), were included on some devices, through a final lithography step followed by metal-liftoff.

Experimental results

Static delay

From Eqn.3, we can see that the shape of the EIT-like peak depends on the phase spacing between the two resonances, which in turn depends on the distance between the two resonators, L , the waveguide dispersion $\beta(\omega)$ and the phase accumulated upon reflection from a cavity. If the cavities have an identical resonance frequency and the condition $2\beta(\omega_0)L = 2n\pi$ is satisfied, then the EIT-like peak is located at ω_0 and is narrow-band and symmetric. As the two cavities are moved away from each other, i.e. L is increased, a broadened, asymmetric peak appears (for resulting phase shifts $< 2\pi$). Fig. 4 shows the normalized transmission spectra through the coupled cavity systems shown in Fig.3c, where the inter-cavity distances are $25\mu m$, $50\mu m$ and $75\mu m$ respectively. The corresponding group delay spectra, obtained

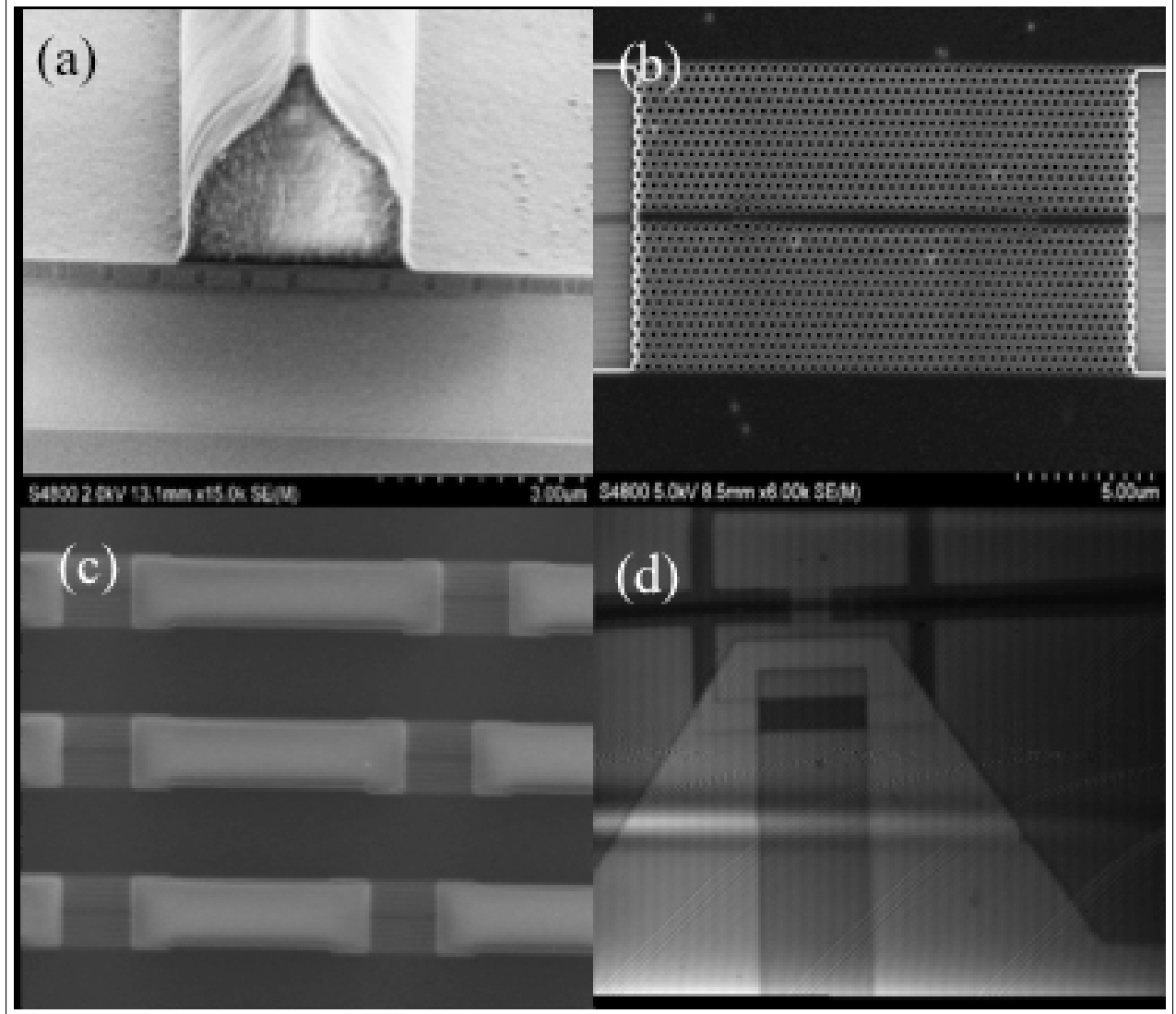


Figure 3: Scanning electron microscope images of the fabricated structures. a) Cross-sectional view of the polymer waveguide above a PhC cavity. b) Top view of a dispersion adapted PhC cavity. c) Three coupled cavity systems, with different inter-cavity distances and d) Ohmic heater next to a PhC cavity.

through a Mach-Zehnder interferometer based Fourier transform spectroscopy approach¹⁶ are shown in Fig.4e-h. All figures are fitted using the same set of Q-factors (with cavity A and B displaying an intrinsic Q-factor of 14000 and 16000 respectively and a coupling Q-factor of 6500 and 7600, respectively. The resonance frequency of each cavity is shown in Table.1. The three separations represent different round trip phases and result in different group delay values, with a maximal value of approximately 200ps. In the case of Fig.4a,b,d and e), the waveguide round trip phase is $2n\pi$ resulting in a strong EIT peak and group delays of 175ps and 200ps respectively. These values exceed the single pass delay of the waveguide sections and the cavities by a factor of 10, indicating that the resonators interfere, producing a strong EIT-analogue effect. The system experiencing a 200ps delay has a on-EIT-peak transmission of 0.5, corresponding to a 3dB loss for 200ps delay and hence a optical loss of only 15dB/ns. In Fig. 4 c) and f) the round trip phase is detuned from $2n\pi$ (370π in this case), resulting in a much weaker EIT-peak and consequently a reduced group delay of only 40ps.

It should be noted that the EIT analogue effect is fundamentally different to traditional slow light mechanisms such as photonic crystal waveguides or Coupled Resonator Optical waveguides.¹⁷

Table 1: **Cavity resonance frequencies for static delay**

ω_a	ω_b
1536.92	1537.31
1537.17	1537.42
1537.12	1537.31

Dynamic delay tuning

In addition to controlling the delay by fixing the intra cavity distance, we can also control the delay by (de)tuning the resonance frequencies of the cavities, providing us with dynamic control over the systems group delay. Here, we incorporated metal contacts and Ohmic heaters for thermal tuning of one cavity resonance, allowing dynamic control over the frequency

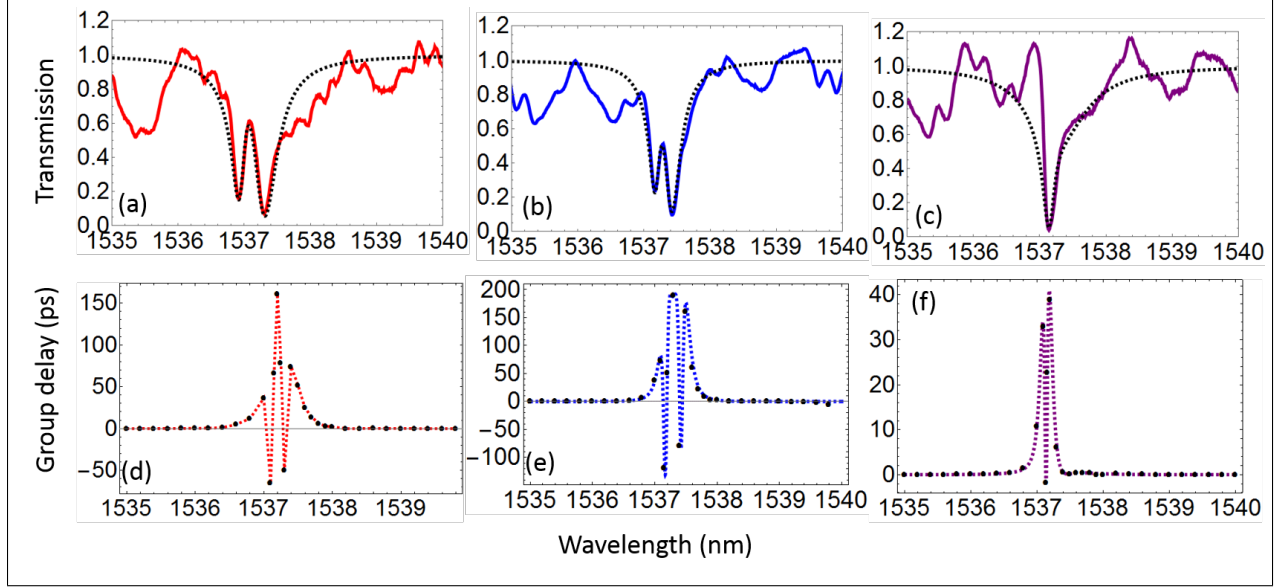


Figure 4: Experimental transmission spectra (solid lines) and theoretical fits (dashed lines), for varying separations (from left to right: 25μm, 50μm and 75μm) between the two coupled cavities in (a)-(c). Experimental group delay spectra (data points) and theoretical fits (dashed lines) are showed in (d)-(f)

detuning. In Fig.5 we show a tuning of the EIT-like transmission spectrum in a two-coupled cavity system, with the cavity parameters listed in Table 2. We tune ω_b , while keeping ω_a constant, thus changing the frequency separation. As thermal tuning is involved, we can only red-shift the cavity resonance, due to the positive thermo-optic coefficient of silicon. In the initial state (0mW power) the resonance of cavity b is slightly blue shifted from the ideal detuning for the (fixed) round trip waveguide phase, $\beta(\omega)L$, separating the two cavities. At this point the system displays a relatively broad transmission window, with a moderate group delay (100-150ps) (Fig.5 a and e). As the electrical power is increased ω_b is red-shifted, approaching the ideal frequency separation for this cavity system. Consequently, the EIT peak narrows and the group delay is increased, reaching a maximal value of approximately 300ps (Fig.5 b and f). As ω_b is increased further, now leading to an increasing frequency detuning away from the ideal position, the EIT-peak broadens once again and the delay is reduced (Fig.5 c,g and d,h). Thus we demonstrate dynamic tuning of the EIT-transmission window and the associated group delay.

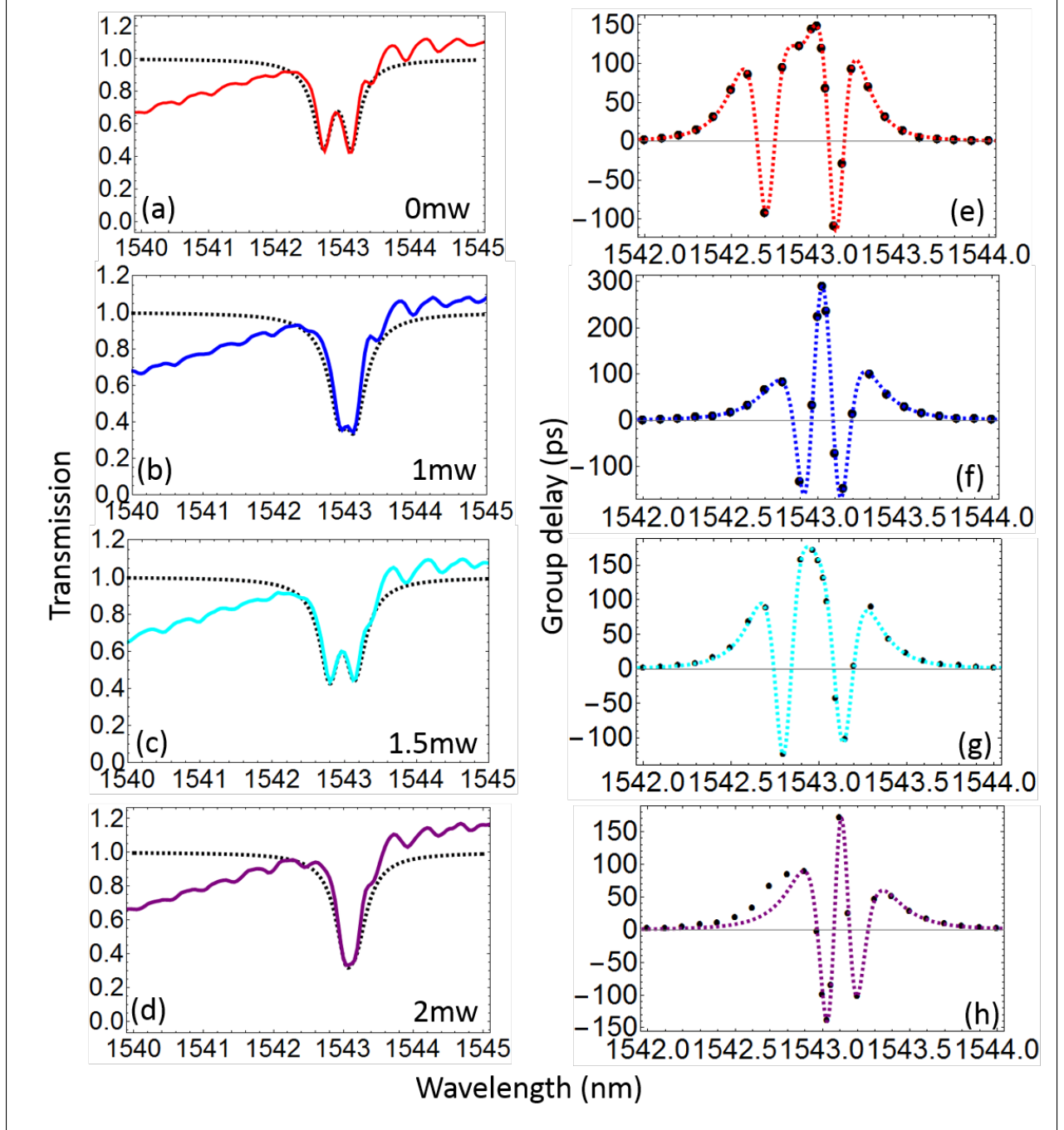


Figure 5: Experimental transmission spectra (solid lines) and theoretical fitting (dashed lines) for a coupled cavity system with different applied heater power a-d. Experimental group delay (data points) and theoretical fit (dashed lines) are shown in panel e-h.

Table 2: **cavity resonance frequencies for dynamic delay tuning**

heater power	ω_a	ω_b
0	1542.825	1543.108
1	1542.830	1543.128
1.5	1542.829	1543.16
2	1542.827	1543.435

An important observation with regards to Table 2 (and this experiment) is as follows. All figures are fitted using the same set of Q-factors (with cavity A and B displaying an intrinsic Q-factor of 14000 and 16000 respectively and a coupling Q-factor of 6500 and 7600, respectively). This is reasonable, as thermo-optic tuning does not introduce optical loss and the frequency shift is extremely small and therefore does not alter the characteristics of the transmission line shape of an individual cavity by itself. Therefore, the change in the line shape (and group delay) of the coupled cavity system comes almost entirely from the changing phase shift experienced upon reflection from the tuned cavity. Since only a single PhC cavity, with a footprint of $\approx 200\mu m^2$ is tuned, this system has a low power consumption. For a slightly better adjusted initial position, i.e. if the cavities were at the ideal frequency detuning to begin with, a modulation of the tuning power by 0.5mW gives a delay tuning of 120ps, as shown in Fig.6.

Discussion and conclusion

From the theoretical descriptions it follows that for a loss-less system (both waveguide and resonators), the EIT peak can be tuned to an arbitrarily narrow bandwidth, resulting in an arbitrarily large delay. However, in reality fabrication imperfections always introduce some loss. The existence of losses will have two main effects, a broadening of the minimal bandwidth to which the EIT peak can be tuned and a reduction of the group delay. Since low-loss operation is desirable, we have chosen the quality factors in our system such that the coupled Q-factor is significantly lower than the intrinsic Q-factor, ensuring that the light is

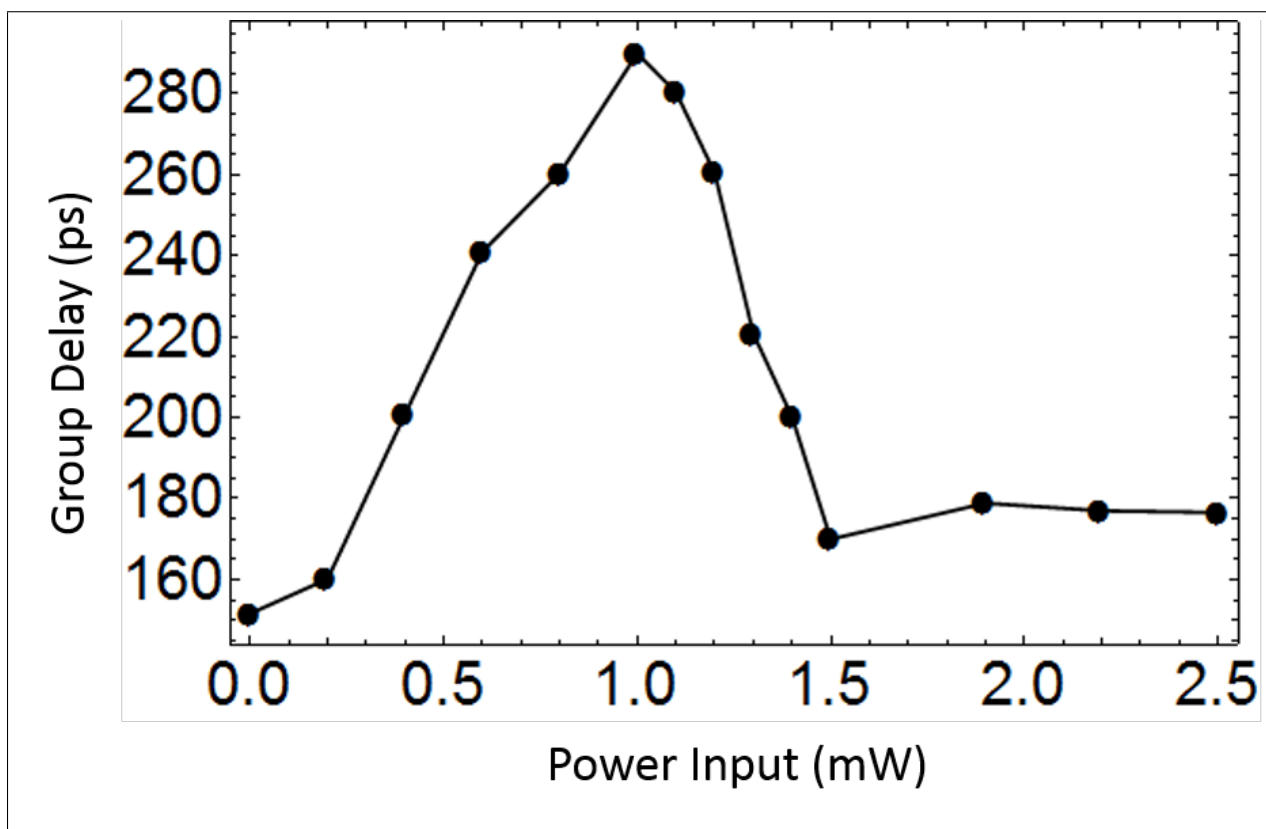


Figure 6: Change in group delay vs heater power for the device from fig.5.

coupled back into the waveguide before it can undergo radiative decay and be lost from the system. Similarly, the polymer waveguide has low propagation loss, ensuring a good cavity-cavity coupling and that light is transmitted through the system before undergoing significant scattering which would result in optical loss. Consequently our device demonstrated a tuning of the delay from 160-300ps (see Fig.6), with an optical loss of roughly 15dB/ns. As our system is based on a resonant effect (and is linear, reciprocal and time-invariant), it follows that like all such systems the device is constrained by the delay-bandwidth limit,¹⁸ which for resonant systems has a maximum value of $\Delta\tau\Delta\omega = 2\pi$. An examination of our measured data reveals a delay-bandwidth product of approximately 5.6, very close to the theoretical maximum. In Table.3 we compare the delay-bandwidth product, the optical loss and the achieved delay of exemplary delay line implementations in silicon photonics. Our system clearly outperforms previous EIT analogue systems with respect to all three figures of merit, while outperforming traditional PhC waveguide or ring resonator CROW based structures with respect to the achieved delay and the propagation loss.

For traveling wave systems, such as slow light waveguides or CROWs, the delay-bandwidth product is a poor figure of merit,^{8,18} since the delay can be increased by increasing the device length, without affecting the bandwidth. In these devices the achievable delay is in fact limited by the propagation loss,⁸ which is fundamentally linked to the refractive index contrast of the materials used. Through the use of a low index polymer waveguide connecting the silicon PhC cavities, we can dramatically outperform pure silicon photonics devices in respect to the propagation loss, while maintaining a large delay and useful delay bandwidth product.

Our achieved delay values do not represent the upper limit of what is possible. For the optimal delay, both cavities should be at exactly the same resonance wavelength (i.e. zero detuning) with a waveguide phase corresponding exactly to $2n\pi$. In our system the maximal delay is achieved for a slightly detuned cavities, indicating a waveguide phase contribution that deviates slightly from the optimum value. Both the initial cavity detuning and the

Table 3: Optical loss, delay and delay-bandwidth product values for difference delay line implementations in silicon photonics. RR indicates structures based on ring resonators and CROW indicates a coupled resonator optical waveguide.

device type	optical loss (dB/ns)	delay (ps)	delay-bandwidth product
this device	15	300	5.6
EIT analogue (L_x PhC cavity) ¹⁹	85	17	0.16
EIT analogue (RR) ¹²	65	30	0.94
PhC waveguide ⁶	35	85	8.5
CROW (RR) ²⁰	100	220	41

deviation of the waveguide phase can be attributed to fabrication imperfections. In a slightly more complex system, three tuning elements could be used to reach the ideal condition. In this case, each cavity could be tuned, to ensure zero frequency detuning and a third element could control the waveguide phase, to ensure that the ideal phase condition is met. Not only would this system allow a larger delay, it would also allow for a larger delay tuning range. The minimum delay of the system is the single pass delay through the waveguide, achieved when both cavities are fully detuned from the operating wavelength. The delay could then be increased by bringing one cavity on resonance. The delay would now be a single pass through waveguide and one cavity. Bringing the second cavity into resonance (but tuning the waveguide phase such that the EIT condition is not met) will lead to a further increase in the system's delay, now corresponding to a single pass through the waveguide and both cavities. Finally, the waveguide phase could be adjusted by tuning the waveguide phase and meeting the EIT condition, providing maximal tuning of the delay. In our demonstration of the above phenomena the cavities were separated by only $350\mu m$ of waveguide. This length of waveguide corresponds to a delay of approximately 2ps. Thus a full control over both cavities would allow for a tuning of the delay from 2ps to over 300ps.

Improvements in the system performance could also be achieved by using PhC cavities with higher intrinsic quality factors, while keeping the cavity to waveguide coupling constant. This would further reduce the percentage of light lost to radiative decay of the cavity modes and therefore reduce the loss and increase the achievable delay. Simulations show that modest

improvements of the intrinsic Q-factor and coupling would allow delays of 1ns or greater to be reached. Additional flexibility and faster tuning speeds can be achieved by replacing the Ohmic heaters with electro-optic tuning, through either carrier injection or depletion. In this case both a red- and blue-shift of the cavity resonance are possible, providing additional freedom in the tuning. Electro-optic modulation also allows for faster tuning than the thermo-optic effect and would therefore be recommended for the integration of the delay line into high-speed communication applications. Replacing the polymer with ultra-low loss silicon nitride waveguides²¹ promises extremely large optical delays. The vertical-coupling scheme employed here is well suited for integration with other optical elements and for electro-optic tuning.^{15,22}

Our system solves the challenge of a compact, low-loss delay line that can be tuned with low power consumption and compares favourable with other delay line implementations across typical figures of merit (optical loss, achieved delay and the delay-bandwidth product). It does so by combining the ideal characteristics of all constituent elements. Polymer waveguides provide very low chip-to-fibre coupling losses and low propagation loss, but on their own have very limited tunability and provide limited delay. Silicon PhC cavities on the other hand provide small footprint solutions, with low power consumption, large tunability and large optical delays, however, the high refractive index contrast leads to poor chip-to-fibre coupling and large scattering losses that limit the maximum delay. By combining both PhC cavities and low loss waveguides we achieve a low-loss, small footprint, low-power tunable optical delay line, with a record low loss (for silicon photonics based structures) of 15dB/ns.

Given the specific distance between two coupled cavities, we find EIT-like phenomena achieved in vertical coupling photonic crystal system, when the phase difference between two cavities is close to $2n\pi$. To effectively control bandwidth of EIT-like peak and group delay, electrical modulation methods based on thermal-effect has been demonstrated to overcome the limitation of bandwidth and single cavity system.

1 Author Contributions

CH designed and simulated the structures, CH and AL fabricated the devices, CH characterised the devices, SAS supervised the device characterisation, CH and SAS analysed the results, LOF supervised all aspects of the project. All authors contributed to the writing of the manuscript and approved the final version.

Acknowledgement

We acknowledge funding from the European Research Council (ERC) under the European Union's Seventh Framework Programme (FP7/2007- 2013) / ERC grant agreement n337508

References

- (1) T.F.Krauss, Why do we need slow light? *Nature Photonics* **2008**, *2*, 448.
- (2) T.Baba, Slow light in photonic crystals. *Nature Photonics* **2008**, *2*, 465.
- (3) Kondo, K.; Shinkawa, M.; Hamachi, Y.; Y.Saito,; Arita, Y.; Baba, T. Ultrafast Slow-Light Tuning Beyond the Carrier Lifetime Using Photonic Crystal Waveguides. *Phys. Rev. Lett.* **2013**, *110*, 053902.
- (4) Hayakawa, R.; Ishikura, N.; Nguyen, H. C.; Baba, T. High-speed delay tuning of slow light in pin-diode-incorporated photonic crystal waveguide. *Optics Letters* **2013**, *38*, 2680.
- (5) Melloni, A.; Morichetti, F.; Ferrari, C.; Martinelli, M. Continuously tunable 1 byte delay in coupled-resonator optical waveguides. *Optics Letters* **2008**, *33*, 2389–2391.
- (6) Melloni, A.; Canciamilla, A.; Morichetti, F.; Ferrari, C.; Martinelli, M.; O’Faolain, L.; Krauss, T. F.; Rue, R. D. L.; Samarelli, A.; Sorel, M. Tunable delay lines in silicon

- photonics: coupled resonators and photonic crystals, a comparison. *IEEE Photonics Journal* **2010**, *2*, 181–194.
- (7) Andrea Melloni, F. M. The long march of slow photonics. *Nature Photonics* **2009**, *3*, 119.
 - (8) Schulz, S. A.; O’Faolain, L.; Beggs, D. M.; White, T. P.; Melloni, A.; Krauss, T. F. Dispersion engineered slow light in photonic crystals: a comparison. *Journal of Optics* **2010**, *12*, 104004.
 - (9) Billings, S.; Schulz, S. A.; Upham, J.; Boyd, R. W. Application-tailored optimisation of photonic crystal waveguides. *Journal of Optics* **2016**, *18*, 115005.
 - (10) M.Minkov;; Savona, V. Wide-band slow light in compact photonic crystal coupled-cavity waveguides. *Optica* **2015**, *2*, 631–634.
 - (11) Giuntoni, I.; Stolarek, D.; Kroushkov, D. I.; Bruns, J.; Zimmermann, L.; Tillack, B.; Petermann, K. Continuously tunable delay line based on SOI tapered Bragg gratings. *Optics Express* **2012**, *20*, 11241–11246.
 - (12) Xu, Q.; Sandhu, S.; Povinelli, M. L.; Shakya, J.; Fan, S.; Lipson, M. Experimental Realization of an On-Chip All-Optical Analogue to Electromagnetically Induced Transparency. *Physical Review Letters* **2006**, *96*, 123901.
 - (13) Smith, D.; Chang, H.; Fuller, K.; Rosenberger, A.; Boyd, R. Coupled-Resonator-Induced Transparency.
 - (14) Welna, K.; Portalupi, S. L.; Galli, M.; O’Faolain, L.; Krauss, T. F. Novel waveguides-adapted photonic crystal cavity with improved disorder stability. *IEEE Journal of Quantum Electronics* **2012**, *48*, 117–1183.
 - (15) Debnath, K.; O’Faolain, L.; Gardes, F. Y.; Steffan, A. G.; Reed, G. T.; Krauss, T. F.

- Cascaded modulator architecture for WDM applications. *Optice Express* **2012**, *20*, 27420–27428.
- (16) Gomez-Iglesias, A.; O’Brien, D.; O’Faolain, L.; Miller, A.; Krauss, T. F. Direct measurement of the group index of photonic crystal waveguides via Fourier transform spectral interferometry. *Appl. Phys. Lett.* **2007**, *90*, 261107.
 - (17) Cardenas, J.; Foster, M. A.; Sherwood-Droz, N.; Poitras, C. B.; Lira, H. L. R.; Zhang, B.; Gaeta, A. L.; Khurgin, J. B.; Morton, P.; Lipson, M. Wide-bandwidth continuously tunable optical delay line using silicon microring resonators. *Optics Express* **2010**, *18*, 26525 – 26534.
 - (18) Tsakmakidis, K.; Shen, L.; Schulz., S. A.; Zheng, X.; Upham, J.; Deng, X.; Altug, H.; Vakakis, A. F.; Boyd, R. W. Breaking Lorentz reciprocity to overcome the time-bandwidth limit in physics and engineering. *Science* **2017**, *356*, 1260–1264.
 - (19) Kocaman, S.; Yang, X.; McMillan, J. F.; Yu, M. B.; Wong, D. L.; Wong, C. W. Observation of temporal group delay in slow-light multiple coupled photonic crystal cavities. *Applied Physics Letters* **2010**, *96*, 221111.
 - (20) F.Xia,; L.Sekaric,; Y.A.Vlasov, Ultracompact optical buffers on a silicon chip. *Nature Photonics* **2006**, *1*, 65.
 - (21) Marpaung, D.; Roeloffzen, C.; Heideman, R.; Leinse, A.; Sales, S.; Capmany, J. Integrated microwave photonics. *Laser and Photonics Reviews* **2013**, *7*, 506–538.
 - (22) Liles, A. A.; Debnath, K.; O’Faolain, L. Lithographic wavelength control of an external cavity laser with a silicon photonic crystal cavity-based resonant reflector. *Optics Letters* **2016**,

Graphical TOC Entry

